

Time Encoding of Finite-Rate-of-Innovation Signals

Abijith Jagannath Kamath, *Student Member, IEEE*, Sunil Rudresh,
and Chandra Sekhar Seelamantula, *Senior Member, IEEE*

Abstract—Time encoding of continuous-time signals is an alternative sampling paradigm to conventional methods like Shannon sampling. In time encoding, the signal is encoded using a sequence of time instants where an event occurs, and hence fall under *event-driven sampling methods*. Time encoding can be designed agnostic to the global clock of the sampling hardware which means the sampling is asynchronous. Moreover, the samples are sparse. This makes time encoding energy efficient. However, the signal representation is nonstandard and in general, nonuniform. In this paper, we consider the extension to time encoding of finite-rate-of-innovation signals, and in particular, periodic signals composed of weighted and time-shifted versions of a known pulse. We consider time encoding using crossing-time-encoding machine (C-TEM) and integrate-and-fire time-encoding machine (IF-TEM). We analyse time encoding in the Fourier domain and arrive at the familiar sum-of-sinusoids structure in the Fourier-series coefficients that can be obtained from the time-encoded measurements via some forward linear transformation, where standard techniques in FRI signal recovery can be applied. Further, we extend this theory to multichannel time encoding such that each channel operates with a lower sampling requirement. We then study the effect of measurement noise, where the temporal measurements are perturbed by additive jitter. To combat the effect of noise, we propose a robust optimisation framework to simultaneously denoise the Fourier-series coefficients and recover the annihilating filter. We provide sufficient conditions for time encoding and perfect reconstruction using C-TEM and IF-TEM, and provide extensive simulations to support our claims.

Index Terms—Time-encoding machines (TEM), finite-rate-of-innovation (FRI) sampling, time-based sampling, crossing-time-encoding machine (C-TEM), integrate-and-fire time-encoding machine (IF-TEM).

I. INTRODUCTION

SAMPLING theory provides an interface between analogue signals and digital processing techniques. Conventionally, uniform samples of the signal or its filtered version provides its discrete representation with perfect recovery guarantees, given sufficient sampling rate, that depends on the class of signals [1]. To this end, Shannon sampling [2] stood as the gold standard for generations, owing to its simplicity and least-squares optimality in classes of nonbandlimited signals. Time encoding is an alternative sampling framework to conventional uniform sampling, where the discrete representation of the signal is a sequence of measurements along its abscissa. These time instants are determined by an event, and in general, generate nonuniformly spaced time instants. The device used to obtain such measurements is called a *time-encoding machine* (TEM). Such sampling methods are motivated from neuroscience

A. J. Kamath and C. S. Seelamantula are with the Department of Electrical Engineering, Indian Institute of Science, Bangalore.

S. Rudresh is with Walmart Global Tech., Bangalore.

For part of this work, S. Rudresh was with the Department of Electrical Engineering, Indian Institute of Science, Bangalore.

where representation of sensory information as a sequence of action potentials is encoded temporally [3], [4]. Lazar and Tóth [5] designed the integrate-and-fire time-encoding machine (IF-TEM) that encodes time instants where the running integral of the signal crosses a threshold. The sampling mechanism is asynchronous, real time implementable, energy efficient and generates sparse measurements. For example, when the signal is a constant, the time instants recorded are farther apart on the average as compared to signals that have higher bandwidth, i.e., there is an intrinsic opportunistic nature of time encoding mechanisms. Such sampling mechanisms fall under the category of event-driven sampling that have made way for a new class of audio and visual sensors that work on the neuromorphic principle [6], [7].

The discrete representation of the signal obtained using the IF-TEM is a sequence of nonuniform time instants called the *trigger times*, along with the corresponding local average values between consecutive trigger times. Signal recovery is a generalised problem of recovery using nonuniform samples of a known transformation of the signal. When the signal is known to be bandlimited, signal recovery from their nonuniform temporal measurements and local averages is solved using an iterative method [8] based on Sandberg's Theorem [9]. The iterations can be viewed as alternating projections onto convex sets (PoCS) [10]. The projections alternate between maintaining measurement consistency and imposing bandlimitedness. The iterations converge when the average sampling rate is greater than the Nyquist rate. Aldroubi and Grochenig [11] have extended this sampling theory to accommodate signals in shift-invariant spaces. In this case, as with bandlimited signals, the recovery algorithm is iterative of the PoCS type and the sampling requirements are of the order of the Nyquist criterion [12].

In this paper, we extend the theory to signals that lie in a union of subspaces [13], and in particular, signals that have finite rate of innovation (FRI) [14]. The FRI model represents sparse analogue signals for which the sampling requirements match the rate of innovation. We consider the prototype τ -periodic FRI signal of the form:

$$x(t) = \sum_{m \in \mathbb{Z}} \sum_{k=0}^{K-1} c_k \varphi(t - t_k - m\tau), \quad (1)$$

where φ is a known pulse and the parameters $\{(c_k, t_k)\}_{k=0}^{K-1}$ are unknowns. The rate of innovation for such signals is $\frac{2K}{\tau}$ and they can be recovered using $2K$ samples in τ -length interval. In the critical case, the pulse maybe a Dirac impulse, in which case, the signal is nonbandlimited. Yet, the minimum sampling requirement is the same. Such sampling frameworks get to be called sub-Nyquist frameworks, and find

applications in RADAR [15], [16], ultrasound imaging [17], radioastronomy [18], etc. Such signals also lie in a union of subspaces where the parameters $\{t_k\}_{k=0}^{K-1}$ defines each subspace. Hence, signal recovery composes of two steps: first, localise the subspace by estimating $\{t_k\}_{k=0}^{K-1}$ and then, second, find the parameters $\{c_k\}_{k=0}^{K-1}$. We consider the reconstruction of FRI signals via parameter estimation from their time-encoded measurements using C-TEM and IF-TEM, and show that the sampling requirements for perfect recovery are of the order of its rate of innovation. We consider the effect of noise on the temporal measurements. This causes the perturbations to appear in the forward linear transformation and the signal measurements. To this end, we propose a optimisation approach that jointly denoises and recovers the parameters. The optimisation programme is similar to Generalised FRI [18], and is solved using alternating minimisation in the joint variables. Further, we show multichannel time encoding can be brought under the same framework, such that each channel can operate with a reduction in the sampling requirement.

A. Related Literature

Alexandru and Dragotti [19] address the problem of recovery of a stream of Dirac impulses from time-encoded measurements. They propose a sequential algorithm to recover a stream of Dirac impulses one at a time. To achieve sequential reconstruction, the interval between two consequent Dirac impulses must be more than the support of the sampling kernel. Therefore, to recover Dirac impulses that are arbitrarily close, the support of the sampling kernel must be arbitrarily small and the sampling kernel becomes signal dependent. Further, to sequentially recover Dirac impulses that are arbitrarily close, the number of samples to be obtained needs to be high. The sampling requirements given for a general FRI signal is higher than the order of the rate of innovation of the signal. This is restricts the class of FRI signals that can be recovered perfectly from time-encoded measurements.

In our work, we analyse the reconstruction in the Fourier domain, where the analysis does not restrict the class of FRI signals and allows using any sampling kernel, independent of the signal. Further, we show that the model extends to general FRI signals of sum of weighted and time-shifted pulses. We then study the effect of noise in the measurements and its effects on the the forward linear transformation as well as the signal measurements. Further, we show this theory extends to multichannel time encoding.

B. Organisation of This Paper

In Section II, we formally introduce time-encoding machines and the mathematical preliminaries. In Section III, we formulate the problem statement. We discuss, time encoding of FRI signals using C-TEM and IF-TEM in Section IV. We extend the formulation to include multichannel time encoding in Section V. In Section VI, we consider the effect of measurement noise and propose an optimisation algorithm for robust signal recovery. We demonstrate the working of the algorithm with experiments in Section VII, and provide concluding remarks in Section VIII.

II. PRELIMINARIES

In this Section, we formally introduce time-encoding machines, in particular, the crossing-time-encoding machine (C-TEM) and the integrate-and-fire time-encoding machine (IF-TEM). We then introduce the Toeplitzification operator and Prony's method which are key to FRI signal processing.

A. Time-Encoding Machines

Time-encoding machines, like the IF-TEM proposed in [5], is a mapping from a function space to a sequence of time instants. Formally:

Definition 1. (Time-encoding machine) Let V be the space of real-valued functions. A time-encoding machine \mathcal{T} with an event operator $\psi : V \rightarrow V$ and references $\{r_i \in V\}_{i \in \mathbb{Z}}$ is a map $\mathcal{T} : V \rightarrow \mathbb{R}^{\mathbb{Z}}$ such that $V \ni y \mapsto \mathcal{T}y$, with:

- a. $\mathcal{T}y = \{t_i \in \mathbb{R} \mid t_i > t_j, \forall i > j, i \in \mathbb{Z}\}$,
- b. $\lim_{n \pm \infty} t_n = \pm\infty$,
- c. $(\psi y)(t_i) = r_i(t_i), \forall t_i \in \mathcal{T}y$.

The output sampling set of a time-encoding machine is a set of “trigger times” of the form $\mathcal{T}y$ which has strictly increasing entries. Such a set $\mathcal{T}y$ is meant to encode the signal y . In the case for uniform sampling, ψ is the identity operator, and the references are signal dependent $r_i(t) = t - (t_{i-1} + T_s) + y(t_i)$, where T_s is the sampling interval. Under most uniform sampling frameworks, perfect reconstruction properties depend on the sampling interval T_s . In the general setting, we define sampling density:

Definition 2. (Sampling density) Let $X = \{t_i \in \mathbb{R}\}_{i \in \mathbb{Z}}$ be a sampling set obtained from a time-encoding machine \mathcal{T} . The sampling density $d(X)$ of X is defined as:

$$d(X) = \sup_{i \in \mathbb{Z}} |t_{i+1} - t_i|. \quad (2)$$

Definition 3. (ϵ -distinct sampling set) Let $X = \{t_i \in \mathbb{R}\}_{i \in \mathbb{Z}}$ be a sampling set obtained from a time-encoding machine \mathcal{T} . The sampling set is said to be ϵ -distinct if $|t_{i+1} - t_i| > \epsilon, \forall t_i \in X, i \in \mathbb{Z}$.

Remark. (Sampling sets from time-encoding machines)

- a. In the case of uniform sampling, the sampling density of the sampling set reduces to the sampling interval T_s , and the sampling set is ϵ -distinct for any $\epsilon < T_s$.
- b. Similar to uniform sampling, we are interested in time-encoding machines that have bounded sampling density and ϵ -distinct.
- c. Although “sampling” using a time-encoding machine of some signal $y \in V$ records only the trigger times in $\mathcal{T}y$, we obtain, via the event operator, samples of the transformed signal $\{(\psi y)(t_i)\}_{i \in \mathbb{Z}}$, which can be computed from the references $\{r_i\}_{i \in \mathbb{Z}}$ via the Definition 1. Hence, the time-encoding machine explicitly gives the sampling set $\{t_i\}_{i \in \mathbb{Z}}$ along with $\{(\psi y)(t_i)\}_{i \in \mathbb{Z}}$, in contrast to the implicit nature of the sampling set in uniform sampling.

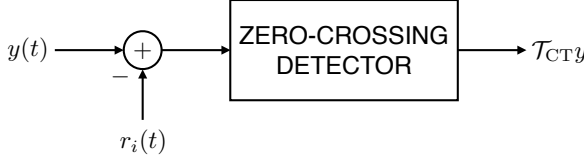


Fig. 1. A schematic of crossing-time-encoding machine with reference r_i .

1) *Crossing-Time-Encoding Machine*: The crossing-time-encoding machine (C-TEM) is a generalised zero crossing detector. The signal to be encoded is matched with a sinusoidal signal and encoded using the time instants where the difference between the signal and the reference crosses zero. Logan [20] studied the encoding of bandlimited signals in its zero-crossings. Encodings of this type are favourable as there are no clipping issues with the dynamic range of the signal to be sampled. However, such encodings are not always invertible. Bar-David [21] showed that the zero-crossings of any bandlimited signal with a sine-wave subtraction of a sufficient frequency is an invertible encoding of the bandlimited signal. Such a sampling mechanism can be interpreted as a time-encoding machine where the signal is matched with a sinusoid. This case, using a sinusoid, is interesting as it ensures bounded sampling density for any input under mild assumptions.

Consider the time-encoding machine \mathcal{T}_{CT} with sinusoidal references $r_i(t) = A_r \cos(2\pi f_r t + \phi_r)$, $\forall i$, and identity event operator $\psi = \text{Id}$. Figure 1 shows the implementation of the C-TEM using a zero-crossing detector. Let y be the input to the C-TEM with reference $r = r_i$. The output of the C-TEM is the set of time instants $\mathcal{T}_{CT}y = \{t'_n \in \mathbb{R} \mid y(t'_n) = r(t'_n), n \in \mathbb{Z}\}$. Using Definition 1, $\mathcal{T}_{CT}y$ can be used to populate the entries in the sequence $\{y(t'_n)\}_{n \in \mathbb{Z}}$ using the reference.

Lemma 1. (Sampling density of C-TEM) Let y be the input to a C-TEM with reference $r(t) = A_r \cos(2\pi f_r t)$. Suppose $A_r \geq \|y\|_\infty$, the output of the C-TEM $\mathcal{T}_{CT}y = \{t'_n \in \mathbb{R} \mid y(t'_n) = s(t'_n), n \in \mathbb{Z}\}$ satisfies $\sup_{n \in \mathbb{Z}} |t'_{n+1} - t'_n| < \frac{1}{f_s}$.

Proof. See Appendix A. \square

2) *Integrate-and-Fire Time-Encoding Machine*: The integrate-and-fire time-encoding machine (IF-TEM) is inspired by representation of sensory information. We use the IF-TEM as designed in [5] without refractory period, as shown in Figure 2. The input is first offset by a constant $b > 0$, and then integrated and scaled by κ . This is compared to a threshold γ and the integrator is reset to zero when the output of the integrator reaches γ . The output of the IF-TEM is a bi-level signal $z(\cdot; \mathcal{T}_{IF}y)$ with transitions at $\mathcal{T}_{IF}y$. We do not address how $\mathcal{T}_{IF}y$ is obtained from $z(\cdot; \mathcal{T}_{IF}y)$ and we refer to methods such as [22]. In this discussion, we assume there is an exact method to obtain $\mathcal{T}_{IF}y$ from $z(\cdot; \mathcal{T}_{IF}y)$ and refer to the set $\mathcal{T}_{IF}y = \{t'_n \in \mathbb{R} \mid n \in \mathbb{Z}\}$ as the output of the IF-TEM.

Lemma 2. (*t*-Transform, cf. [5]) Let y be the input to an IF-TEM with parameters $\{b, \kappa, \gamma\}$ as shown in Figure 2. The

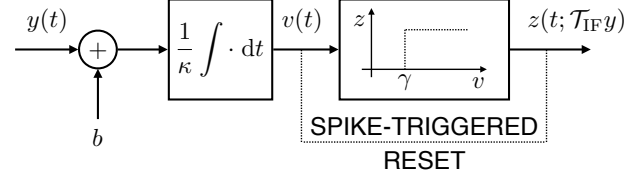


Fig. 2. A schematic of integrate-and-fire time-encoding machine with parameters $\{b, \kappa, \gamma\}$.

output of the IF-TEM is a strictly increasing set of time instants $\mathcal{T}_{IF}y = \{t'_n \in \mathbb{R}\}_{n \in \mathbb{Z}}$ such that:

$$\bar{y}_n = \int_{t'_n}^{t'_{n+1}} y(t) dt = -b(t'_{n+1} - t'_n) + \kappa\gamma, \forall n \in \mathbb{Z}. \quad (3)$$

Proof. See Appendix B. \square

Lemma 2 defines the event operator for the IF-TEM, using which we populate the sequence $\{\bar{y}_n\}_{n \in \mathbb{Z}}$, given the output of the IF-TEM $\mathcal{T}_{IF}y$.

Corollary 1. (Sampling sets of IF-TEM, cf. [5]) Let y be the input to an IF-TEM with parameters $\{b, \kappa, \gamma\}$ as shown in Figure 2, with $\|y\|_\infty < b$. The output of the IF-TEM $\mathcal{T}_{IF}y = \{t'_n \in \mathbb{R}\}$ satisfies:

$$\frac{\kappa\gamma}{b + \|y\|_\infty} \leq t'_{n+1} - t'_n \leq \frac{\kappa\gamma}{b - \|y\|_\infty}. \quad (4)$$

Proof. See Appendix C. \square

Corollary 1 gives an upper bound on the sampling density for any input. Further, it also guarantees the sampling sets are ϵ -distinct for $\epsilon < \frac{\kappa\gamma}{b + \|y\|_\infty}$.

B. Toeplitzification Operator

Consider the vectors $\mathbf{x} = [x_{-M} \ x_{-M+1} \ \cdots \ x_M]^\top \in \mathbb{C}^N$ and $\mathbf{u} \in \mathbb{C}^{P+1}$. The convolution of the sequences $\tilde{\mathbf{x}} = [\cdots \ 0 \ x_{-M} \ \cdots \ \boxed{x_0} \ \cdots \ x_M \ 0 \ \cdots] \in \mathbb{C}^{\mathbb{Z}}$ and $\tilde{\mathbf{u}} = [\cdots \ \boxed{0} \ u_1 \ \cdots \ u_{P+1} \ 0 \ \cdots] \in \mathbb{C}^{\mathbb{Z}}$ can be presented as a matrix-vector product with \mathbf{u} and a Toeplitz matrix constructed using the entries of \mathbf{x} .

Definition 4. (Toeplitzification Operator) Let $\mathbf{x} \in \mathbb{C}^N$, $N = 2M + 1$, for some $M \in \mathbb{N}$ with entries indexed as $\mathbf{x} = [x_{-M} \ x_{-M+1} \ \cdots \ x_{M-1} \ x_M]^\top$, and consider the set of Toeplitz matrices $\mathbb{T}_P \subset \mathbb{C}^{(N-P) \times (P+1)}$. Then, for any $P \leq M$, \mathbf{x} can be embedded into a Toeplitz matrix in $\mathbb{C}^{(N-P) \times (P+1)}$, using the Toeplitzification operator, $T_P : \mathbb{C}^N \rightarrow \mathbb{T}_P$, with $\mathbf{x} \mapsto (T_P \mathbf{x})_{i,j} = x_{-M+P+i-j}$, $i = 1, \dots, N - P$, $j = 1, \dots, P + 1$.

Remark. (Properties of T_P)

- a. $T_P \mathbf{x}$ is a Toeplitz matrix as the entry at (i, j) depends on $i - j$. The vector \mathbf{x} is called the generator of the matrix $T_P \mathbf{x}$.
- b. $(T_P \mathbf{x}) \mathbf{u}$ denotes the valid part of the convolution between $\tilde{\mathbf{x}}$ and $\tilde{\mathbf{u}}$.
- c. In the case where $P = M$, there exists an operator $R_N : \mathbb{C}^{P+1} \mapsto \mathbb{C}^{(P+1) \times N}$, which is the right dual of T_P , such that $(T_P \mathbf{x}) \mathbf{u} = (R_N \mathbf{u}) \mathbf{x}$, $\forall \mathbf{x}, \mathbf{u}$.

The right dual utilises commutativity of the convolution operation $\tilde{\mathbf{x}} * \tilde{\mathbf{u}} = \tilde{\mathbf{u}} * \tilde{\mathbf{x}}$, and allows the interchange of variables \mathbf{x} and \mathbf{u} .

C. Prony's Method

Consider a τ -periodic stream of Dirac impulses $x(t) = \sum_{m \in \mathbb{Z}} \sum_{k=0}^{K-1} c_k \delta(t - t_k - m\tau)$. Using Poisson summation formula the Fourier-series coefficients are revealed as:

$$x(t) = \sum_{m \in \mathbb{Z}} \frac{1}{\tau} \underbrace{\sum_{k=0}^{K-1} c_k e^{-j2\pi m t_k / \tau} e^{j2\pi m t / \tau}}_{\hat{x}_m}. \quad (5)$$

The Fourier-series coefficients are a linear combination of complex sinusoids or in the sum-of-weighted-complex-exponentials (SWCE) form. The estimation of the parameters $\{t_k\}_{k=0}^{K-1}$ from the Fourier-series coefficients is a spectral estimation problem. Prony's method [23] is a high-resolution spectral estimation (HRSE) technique that uses the SWCE structure of the Fourier-series coefficients. The parameters $\{t_k\}_{k=0}^{K-1}$ can be recovered from $2K + 1$ contiguous Fourier-series coefficients using a $K + 1$ -tap annihilating filter $\mathbf{h} = [\dots 0 \ h_0 \ \dots \ h_K \ 0 \ \dots]$ with roots $\{u_k = e^{-j2\pi t_k / \tau}\}_{k=0}^{K-1}$. The Z-transform of the annihilating filter $H(z) = \sum_{k=0}^K h_k z^{-k} = h_0 \prod_{k=1}^K (1 - u_k z^{-1})$. We have:

$$\begin{aligned} (\mathbf{h} * \hat{\mathbf{x}})(m) &= \sum_{k=0}^K h_k \hat{x}_{m-k} = \sum_{k=0}^K h_k \frac{1}{\tau} \sum_{k'=0}^{K-1} c_{k'} u_{k'}^{(m-k)}, \\ &= \frac{1}{\tau} \sum_{k'=0}^{K-1} c_{k'} u_{k'}^m \underbrace{\sum_{k=0}^K h_k u_{k'}^{-k}}_{H(u_{k'})=0} = 0, \quad \forall m \in \mathbb{Z}. \end{aligned} \quad (6)$$

Using the equations for $m = -M + K, -M + K + 1, \dots, M$, for some $M \geq K$, we get the linear system of equations $(T_K \hat{\mathbf{x}}) \mathbf{h} = \mathbf{0}$, where $\hat{\mathbf{x}} = [\hat{x}_{-M} \ \dots \ \hat{x}_M]^\top \in \mathbb{C}^N$ is the vector of Fourier-series coefficients, and $\mathbf{h} = [h_0 \ \dots \ h_K]^\top \in \mathbb{C}^{K+1}$ contains the coefficients of the annihilating filter.

The annihilating filter is a nontrivial vector in the null space of $T_K \hat{\mathbf{x}}$. For $M \geq K$, since the Fourier-series is a degree- K trigonometric polynomial, it can be shown that $\text{rank}(T_K \hat{\mathbf{x}}) = K$. In fact, for $K \leq P \leq M$, it can be shown that $\text{rank}(T_P \hat{\mathbf{x}}) = K$, and hence a $P + 1$ -tap annihilating filter $\tilde{\mathbf{h}}$ can be found with roots $\{u_k = e^{-j2\pi t_k / \tau}\}_{k=0}^{K-1}$ in the null space of $T_P \hat{\mathbf{x}}$. Although, in this case, the annihilating filter is not unique since the dimension of null space is $P + 1 - K$. However, all solutions are valid [24]. The annihilating filter is found in the null space of $T_P \hat{\mathbf{x}}$ using the Eckart-Young Theorem, that selects the right eigenvector corresponding to the smallest singular value in the singular-value decomposition of the matrix $T_P \hat{\mathbf{x}}$. The roots of the annihilating filter are in one-to-one correspondence with the parameters $\{t_k\}_{k=0}^{K-1}$, and therefore they can be uniquely determined using the annihilating filter.

III. PROBLEM FORMULATION

Let $\varphi \in L^2(\mathbb{R})$ be given. The signal φ maybe the model for a prototype test signal or pulse to be sent at the receiver. Consider the τ -periodic signal $x \in L^2([0, \tau])$:

$$x(t) = \sum_{m \in \mathbb{Z}} \sum_{k=0}^{K-1} c_k \varphi(t - t_k - m\tau), \quad (7)$$

where $\{c_k \in \mathbb{R}\}_{k=0}^{K-1}$ are unknown amplitudes and $\{t_k \in \mathbb{R} \mid 0 < t_1 < t_2 < \dots < t_K < \tau\}_{k=0}^{K-1}$ are the shifts that parametrise the support of the signal. It is clear from the definition that x has a rate of innovation of $\frac{2K}{\tau}$ and therefore, the minimum sampling requirement is $2K$ samples in every period τ .

Since $x \in L^2([0, \tau])$, using Fourier series representation, $\exists! \{\hat{x}_m\}_{m \in \mathbb{Z}}$ such that $x(t) = \sum_{m \in \mathbb{Z}} \hat{x}_m e^{j\omega_0 m t}$, where $\omega_0 = \frac{2\pi}{\tau}$.

Using (7) and Poisson summation formula, the Fourier-series coefficients, similar to (5):

$$\hat{x}_m = \frac{1}{\tau} \hat{\varphi}(m\omega_0) \sum_{k=0}^{K-1} c_k e^{-j\omega_0 m t_k}, \quad (8)$$

where $\hat{\varphi}$ is the Fourier transform of the pulse φ . The Fourier series coefficients admit an SWCE form. The estimation of the shifts from the Fourier-series coefficients, from Section II-C, is achieved with $2K + 1$ contiguous samples of $\left\{ \frac{\hat{x}_m}{\hat{\varphi}(m\omega_0)} \right\}_{m \in \mathbb{Z}}$ using Prony's method [23].

We consider kernel-based time encoding of the τ -periodic FRI signal x , using some sampling kernel g and some time-encoding machine to give the set of time instants $\mathcal{T}y = \{t'_n\}_{n \in \mathbb{Z}}$ and their corresponding signal measurements $\{(\psi y)(t'_n)\}_{n \in \mathbb{Z}}$, where $y = x * g$. We pose the reconstruction problem: given $\mathcal{T}y$, find the FRI signal (7) or equivalently, find the amplitudes and shifts.

IV. TIME ENCODING OF FRI SIGNALS

Using Prony's method in Section II-C, we recover the parameters of the FRI signal (7) from $2K + 1$ contiguous Fourier-series coefficients. In this Section, we analyse the recovery of Fourier-series coefficients from the time encoding of the signal. As in conventional FRI sampling, we propose kernel-based time encoding of the signal x in (7) to 1) spread the signal energy so as to record meaningful samples and 2) obtain the Fourier-series coefficients via a linear system

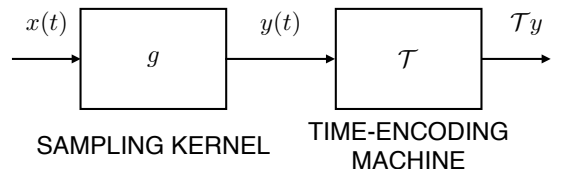


Fig. 3. A schematic of kernel-based time encoding of x using a sampling kernel g and time-encoding machine \mathcal{T} .

of equations. Consider filtering the FRI signal using some sampling kernel g to get $y = x * g$ as:

$$\begin{aligned} y(t) &= (x * g)(t) = \int_{\mathbb{R}} g(\nu) x(t - \nu) d\nu, \\ &\stackrel{(a)}{=} \int_{\mathbb{R}} g(\nu) \sum_{m \in \mathbb{Z}} \hat{x}_m e^{j\omega_0 m(t-\nu)} d\nu, \\ &\stackrel{(b)}{=} \sum_{m \in \mathbb{Z}} \hat{x}_m \left(\int_{\mathbb{R}} g(\nu) e^{-j\omega_0 m\nu} d\nu \right) e^{j\omega_0 mt}, \\ &\stackrel{(c)}{=} \sum_{m \in \mathbb{Z}} \hat{x}_m \hat{g}(m\omega_0) e^{j\omega_0 mt}, \end{aligned} \quad (9)$$

where (a) uses the Fourier-series representation of x , (b) is obtained by interchanging the summation and the integral and (c) is obtained by defining the Fourier transform of the sampling kernel \hat{g} . The filtered signal $y = x * g$ is also a τ -periodic signal with Fourier-series coefficients $\{\hat{x}_m \hat{g}(m\omega_0)\}_{m \in \mathbb{Z}}$. Let the sampling kernel satisfy alias-cancellation conditions, i.e., the sampling kernel g is constructed such that:

$$\hat{g}(m\omega_0) = \begin{cases} g_m \neq 0, & m \in \mathcal{M}, \\ 0, & m \notin \mathcal{M} \\ \text{arbitrary,} & \text{otherwise,} \end{cases} \quad (10)$$

where $\mathcal{M} = -M, \dots, -1, 0, 1, \dots, M$ for some $M \in \mathbb{N}$ with $\text{card}(\mathcal{M}) = 2M + 1$. It is possible to construct such kernels, for example, by choosing a sinc function of bandwidth $2M + 1$, where $g_m = 1, \forall m \in \mathcal{M}$. Other examples for such kernels are: sum of sincs (SoS) kernels in the Fourier domain [17], sum of modulated splines (SMS) kernels in the time domain [25], exponential- and polynomial-reproducing kernels [26], which satisfy the generalised Strang-Fix conditions. Under these conditions, and setting $g_m = 1, \forall m \in \mathcal{M}$ without loss of generality:

$$y(t) = (x * g)(t) = \sum_{m=-M}^M \hat{x}_m e^{j\omega_0 mt}, \quad (11)$$

is a trigonometric polynomial. Such a finite sum makes it possible to construct linear systems that can solve for the Fourier coefficients $\{\hat{x}_m\}_{m=-M}^M$ using $\mathcal{T}y$ and $(\psi y)(\mathcal{T}y)$. In the case of uniform sampling with critical sampling rate, the forward transformation is the discrete-Fourier-transform (DFT) matrix. We investigate the sampling and reconstruction, first using a C-TEM and then using an IF-TEM, to show, under both cases, the Fourier-series coefficients are related to the measurements by a linear transformation.

A. Time Encoding using C-TEM

Let $\mathcal{T}_{CT}y = \{t'_n \in \mathbb{R} \mid y(t'_n) = r(t'_n), n \in \mathbb{Z}\}$ be the output of the C-TEM with sinusoidal reference $r(t) = A_r \cos(2\pi f_r t)$ and the filtered signal $y = x * g$ as the input. Using the reference and Definition 1, under the identity event operator, we have signal measurements:

$$y(t'_n) = \sum_{m=-M}^M \hat{x}_m e^{j\omega_0 mt'_n}, \forall n \in \mathbb{Z}. \quad (12)$$

Let $L \in \mathbb{N}$ measurements be taken in the interval $[0, \tau]$. We obtain a linear system of the form $\mathbf{y} = \mathbf{G}_{CT}\hat{\mathbf{x}}$, using (12), where $\mathbf{y} = [y(t'_1) \ y(t'_2) \ \dots \ y(t'_L)]^T \in \mathbb{R}^L$, $\hat{\mathbf{x}} = [\hat{x}_{-M} \ \dots \ \hat{x}_M]^T \in \mathbb{C}^N$, and $\mathbf{G}_{CT} \in \mathbb{C}^{L \times N}$ as defined in (13).

$$\mathbf{G}_{CT} = \begin{bmatrix} e^{-jM\omega_0 t'_1} & \dots & e^{-j\omega_0 t'_1} & 1 & e^{j\omega_0 t'_1} & \dots & e^{jM\omega_0 t'_1} \\ e^{-jM\omega_0 t'_2} & \dots & e^{-j\omega_0 t'_2} & 1 & e^{j\omega_0 t'_2} & \dots & e^{jM\omega_0 t'_2} \\ \vdots & & \vdots & \vdots & \vdots & & \vdots \\ e^{-jM\omega_0 t'_L} & \dots & e^{-j\omega_0 t'_L} & 1 & e^{j\omega_0 t'_L} & \dots & e^{jM\omega_0 t'_L} \end{bmatrix}, \quad (13)$$

Lemma 3. (Rank properties of \mathbf{G}_{CT}) The matrix $\mathbf{G}_{CT} \in \mathbb{C}^{L \times N}$ defined in (13) has full column-rank whenever $L \geq N$.

Proof. See Appendix D. \square

Note that \mathbf{G}_{CT} reduces to the DFT matrix when the trigger times are uniformly spaced, i.e. $t'_n = nT_s$, where T_s is the sampling interval. \mathbf{G}_{CT} is also the forward linear transformation under random sampling. In this case, the forward linear transformation is invertible whenever the sampling instants are distinct. Hence, the C-TEM may also be viewed as a structured method to obtain nonuniform samples.

Using Lemma 3, with $L \geq N$, the matrix \mathbf{G}_{CT} is left invertible and the solution to the linear system $\mathbf{y} = \mathbf{G}_{CT}\hat{\mathbf{x}}$ is unique. We then use Prony's method discussed in Section II-C to solve for the shifts. Then, the linear system in (8) can be solved using linear least-squares to find the amplitudes.

Proposition 1. (Sufficient conditions for recovery of (7) from C-TEM measurements) Let the τ -periodic FRI signal x in (7) be encoded using a C-TEM with reference r and a sampling kernel g that satisfies (10). The set of time instants $\{t'_n\}_{n=1}^L \subset \mathcal{T}_{CT}(x * g) \cap [0, \tau]$ is a sufficient representation of x when $L \geq 2K + 1$ and the reference is a sinusoid $r(t) = A_r \cos(2\pi f_r t)$ with $A_r > \|x * g\|_{\infty}$ and $f_s \geq \frac{2K + 1}{T_0}$.

Proof. See Appendix E. \square

B. Time Encoding using IF-TEM

Let $\mathcal{T}_{IF}y = \{t'_n \in \mathbb{R} \mid y(t'_n) = r(t'_n), n \in \mathbb{Z}\}$ be the output of the IF-TEM with parameters $\{b, \kappa, \gamma\}$ and the filtered signal $y = x * g$ as the input. Using Lemma 2, we have signal measurements of the form:

$$\begin{aligned} \bar{y}_n &= \sum_{m=-M}^M \frac{1}{j\omega_0 m} \hat{x}_m \left(e^{j\omega_0 mt'_{n+1}} - e^{j\omega_0 mt'_n} \right) \\ &\quad + \hat{x}_0 (t'_{n+1} - t'_n); n = 1, 2, \dots, L - 1, \end{aligned} \quad (14)$$

where $L \in \mathbb{N}$ is the number of measurements in the interval $[0, \tau]$. We obtain a linear system of the form $\bar{\mathbf{y}} = \mathbf{G}_{IF}\hat{\mathbf{x}}$, $\bar{\mathbf{y}} = [\bar{y}_1 \ \bar{y}_2 \ \dots \ \bar{y}_{L-1}]^T \in \mathbb{R}^{L-1}$, $\hat{\mathbf{x}} = [\hat{x}_{-M} \ \dots \ \hat{x}_M]^T \in \mathbb{C}^N$, and $\mathbf{G}_{IF} \in \mathbb{C}^{(L-1) \times N}$ as defined in (15).

$$\mathbf{G}_{\text{IF}} = \begin{bmatrix} e^{-jM\omega_0 t'_2} - e^{-jM\omega_0 t'_1} & \dots & e^{-j\omega_0 t'_2} - e^{-j\omega_0 t'_1} & t'_2 - t'_1 & e^{j\omega_0 t'_2} - e^{j\omega_0 t'_1} & \dots & e^{jM\omega_0 t'_2} - e^{jM\omega_0 t'_1} \\ e^{-jM\omega_0 t'_3} - e^{-jM\omega_0 t'_2} & \dots & e^{-j\omega_0 t'_3} - e^{-j\omega_0 t'_2} & t'_3 - t'_2 & e^{j\omega_0 t'_3} - e^{j\omega_0 t'_2} & \dots & e^{jM\omega_0 t'_3} - e^{jM\omega_0 t'_2} \\ \vdots & \vdots & \vdots & \vdots & \vdots & \vdots & \vdots \\ e^{-jM\omega_0 t'_L} - e^{-jM\omega_0 t'_{L-1}} & \dots & e^{-j\omega_0 t'_L} - e^{-j\omega_0 t'_{L-1}} & t'_L - t'_{L-1} & e^{j\omega_0 t'_L} - e^{j\omega_0 t'_{L-1}} & \dots & e^{jM\omega_0 t'_L} - e^{jM\omega_0 t'_{L-1}} \end{bmatrix} \quad (15)$$

Lemma 4. (Rank properties of \mathbf{G}_{IF}) The matrix $\mathbf{G}_{\text{IF}} \in \mathbb{C}^{(L-1) \times N}$ defined in (15) has full column-rank whenever $L \geq N + 1$.

Proof. See Appendix F. \square

Using Lemma 4, with $L \geq N + 1$, the matrix \mathbf{G}_{IF} is left-invertible and the solution to the linear system $\bar{\mathbf{y}} = \mathbf{G}_{\text{IF}}\hat{\mathbf{x}}$ is unique. We then use Prony's method discussed in Section II-C to solve for the shifts. Then, the linear system in (8) can be solved using linear least-squares to find the amplitudes.

Proposition 2. (Sufficient conditions for recovery of (7) from IF-TEM measurements) Let the τ -periodic FRI signal x in (7) be encoded using an IF-TEM with parameters $\{b, \kappa, \gamma\}$ as in Figure 2 and a sampling kernel g that satisfies (10). The set of time instants $\{t'_n\}_{n=1}^L \subset \mathcal{T}_{\text{IF}}(x * g) \cap [0, \tau[$ is a sufficient representation of x with $(L-1) \geq (2K+1)$ if the parameters of the IF-TEM satisfy:

$$\frac{\kappa\gamma}{b - \|x * g\|_\infty} < \frac{\tau}{L}.$$

Proof. See Appendix G. \square

V. MULTICHANNEL TIME ENCODING OF FRI SIGNALS

The sufficient condition in Proposition 1 often results in obtaining more samples than the rate of innovation of the signal. The sampling requirement on the hardware maybe reduced by using multiple channels. Consider kernel-based time encoding a τ -periodic FRI signal as in (7) using C time-encoding machines $\mathcal{T}^{(1)}, \mathcal{T}^{(2)}, \dots, \mathcal{T}^{(C)}$ and a sampling kernel g that satisfies (10) as shown in Figure 4.

Consider time encoding using C C-TEMs, where each channel has the reference $r^{(c)}(t) = A_r^{(c)} \cos(2\pi f_r^{(c)} t + \phi_r^{(c)})$, $c = 1, 2, \dots, C$. The output of the c th channel is the set of time instants $\mathcal{T}_{\text{CT}}^{(c)} y = \{t_n^{(c)} \in \mathbb{R} \mid y(t_n^{(c)}) = r^{(c)}(t_n^{(c)}), n \in \mathbb{Z}\}$ and samples of the signal $\{y(t_n^{(c)})\}_{n \in \mathbb{Z}}$ obtained using the references and Definition 1. Let $L^{(c)}$ be

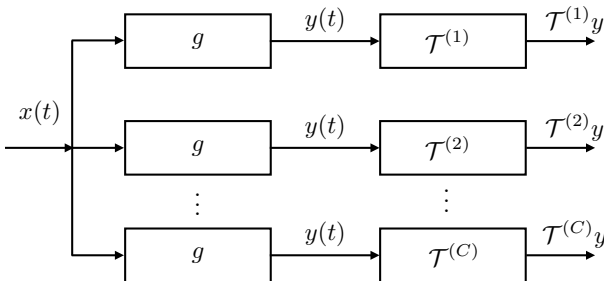


Fig. 4. A schematic of kernel-based multichannel time encoding of x using a sampling kernel g and time-encoding machines $\mathcal{T}^{(1)}, \dots, \mathcal{T}^{(C)}$.

the number of samples recorded by the c th channel in the interval $[0, \tau[$. Similar to (12), each channel constructs a linear system $\mathbf{y}^{(c)} = \mathbf{G}_{\text{CT}}^{(c)} \hat{\mathbf{x}}$ where $\hat{\mathbf{x}} = [\hat{x}_{-M} \dots \hat{x}_M]^\top \in \mathbb{C}^N$, $\mathbf{y}^{(c)} = [y(t_1^{(c)}) \dots y(t_{L^{(c)}}^{(c)})]^\top \in \mathbb{C}^{L^{(c)}}$ and $\mathbf{G}_{\text{CT}}^{(c)} \in \mathbb{C}^{L^{(c)} \times N}$ defined similar to (13).

Similarly, consider time encoding using C IF-TEMs. where each channel has parameters $b^{(c)}, \kappa^{(c)}$ and $\gamma^{(c)}$, $c = 1, 2, \dots, C$ and potentially different initial value for the integrators. The output of the c th channel is the set of time instants $\mathcal{T}_{\text{IF}}^{(c)} y = \{t_n^{(c)}\}_{n \in \mathbb{Z}}$ that satisfy Lemma 2 and Corollary 1 and local averages $\{\bar{y}_n^{(c)}\}_{n \in \mathbb{Z}}$ obtained using Lemma 2. Let $L^{(c)}$ be the number of samples recorded by the c th channel. Similar to (14), each channel constructs a linear system $\bar{\mathbf{y}}^{(c)} = \mathbf{G}_{\text{IF}}^{(c)} \hat{\mathbf{x}}$ where $\hat{\mathbf{x}} = [\hat{x}_{-M} \dots \hat{x}_M]^\top \in \mathbb{C}^N$, $\bar{\mathbf{y}}^{(c)} = [\bar{y}_1^{(c)} \dots \bar{y}_{L^{(c)}}^{(c)}]^\top \in \mathbb{C}^{L^{(c)}}$ and $\mathbf{G}_{\text{IF}}^{(c)} \in \mathbb{C}^{(L^{(c)}-1) \times N}$ defined similar to (15).

In both cases, we use the C linear systems to form a concatenated system as:

$$\underbrace{\begin{bmatrix} \mathbf{y}^{(1)} \\ \mathbf{y}^{(2)} \\ \vdots \\ \mathbf{y}^{(C)} \end{bmatrix}}_{\mathbf{y}} = \underbrace{\begin{bmatrix} \mathbf{G}^{(1)} \\ \mathbf{G}^{(2)} \\ \vdots \\ \mathbf{G}^{(M)} \end{bmatrix}}_{\mathbf{G}} \hat{\mathbf{x}}. \quad (16)$$

The system will admit a unique solution $\hat{\mathbf{x}}$ when \mathbf{G} has full column-rank. This happens when the matrix is tall and when no two channels identically sample the same time instants. This can be achieved easily by setting different phase difference $\phi^{(c)} \in [0, 2\pi[$ of the references in case of sampling using C-TEMs and setting different initial values of the integrator in case of sampling using IF-TEMs. Then, each channel can sample at $\frac{1}{C}$ times the rate such that $\sum_{c=1}^C L^{(c)} \geq (2M+1)$.

In the case of sampling using C C-TEMs, reduction in the sampling requirement can be achieved by reducing the frequency of the reference.

Proposition 3. (Sufficient conditions for recovery of (7) from C C-TEM channels) Let the τ -periodic FRI signal x in (7) be encoded using C C-TEMs with reference $r^{(c)}$ and a sampling kernel g that satisfies (10). The set of C time instants $\{t_n^{(c)}\}_{n=1}^{L^{(c)}} \subset \mathcal{T}_{\text{CT}}^{(c)}(x * g) \cap [0, \tau[, c = 1, 2, \dots, C$ is a sufficient representation of x , when the reference of the c th channel $r^{(c)}(t) = A_r^{(c)} \cos(2\pi f_r^{(c)} t + \phi^{(r)})$ satisfies $A_r^{(c)} \geq \|x * g\|_\infty$ and $f_r^{(c)} \geq \frac{2K+1}{C\tau}$, $\forall c$.

In the case of sampling using C IF-TEMs, reduction in the sampling requirement can be achieved by aiming to measure

$L^{(c)}/C$ samples in the c th channel. Similar to Proposition 2, we have:

Proposition 4. (Sufficient conditions for recovery of (7) from M IF-TEM channels) Let the τ -periodic FRI signal x in (7) be encoded using an IF-TEM with parameters $\{b^{(c)}, \kappa^{(c)}, \gamma^{(c)}\}$ as in Figure 2 and a sampling kernel g that satisfies (10). The set of C time instants $\{t_n'^{(c)}\}_{n=1}^{L^{(c)}} \subset \mathcal{T}_{\text{IF}}^{(c)}(x * g) \cap [0, \tau]$, $c = 1, 2, \dots, C$ is a sufficient representation of x with $(\sum_{c=1}^C L^{(c)} - C) \geq (2K + 1)$ if the parameters of the c th channel satisfy:

$$\frac{\kappa^{(c)} \gamma^{(c)}}{b^{(c)} - \|x * g\|_\infty} < \frac{C\tau}{L^{(c)}}.$$

VI. FRI SIGNAL RECOVERY IN THE PRESENCE OF NOISE

In this section, we consider the effect of measurement noise. In practice, the output obtained from the time-encoding machines like the C-TEM and the IF-TEM shown in Figures 1 and 2 are not sequences of time instants. For example, the crossing times from a C-TEM use root finding algorithms, or in case of the IF-TEM, the output is a bi-level signal that transitions at the trigger times. The trigger times are obtained from such outputs using estimation methods like in [22]. The estimation methods are prone to error. Further, the hardware used to encode the trigger times additionally introduce errors. We model the noise on the trigger times as jitter, i.e., the noisy measurements obtained from time-encoding machines are of the form:

$$\tilde{t}_n' = t_n' + \nu_n, \quad (17)$$

where the noise $\nu_n \stackrel{\text{i.i.d.}}{\sim} \mathcal{U}[-\frac{\sigma}{2}, \frac{\sigma}{2}]$ is modelled to be independent and identically distributed uniform random variables with zero mean and variance $\frac{\sigma^2}{12}$. Unlike in conventional uniform sampling where the noise in the measurements correspond only to the signal measurements, here, the noise in the temporal measurements carry over to perturbations in the signal measurements and the forward linear transformation, as they both depend on the temporal measurements.

Consider kernel-based time encoding of the FRI signal in (7) using a C-TEM with sinusoidal reference $r(t) = A_r \cos(2\pi f_r t)$ that provides noisy trigger times as in (17). The signal samples computed using the reference $y(\tilde{t}_n') = r(\tilde{t}_n') = r(t_n' + \nu_n)$. Since the reference is continuous and differentiable, using the mean value theorem, there exists $t_n^* \in [t_n', t_n' + \nu_n]$ such that, $y(\tilde{t}_n') = r(t_n') + r'(t_n^*)\nu_n$. Hence, the samples of the signal are random variables with $\mathbb{E}[y(\tilde{t}_n')] = \mathbb{E}[r(t_n') + r'(t_n^*)\nu_n] = r(t_n')$, and $\text{var}(y(\tilde{t}_n')) = \text{var}(r(t_n') + r'(t_n^*)\nu_n) = |r'(t_n^*)|^2 \frac{\sigma^2}{12} \leq (2\pi A_r f_r)^2 \frac{\sigma^2}{12}$. Since the variance of the signal measurements depends on the point t_n^* , the distributions of the signal samples are not identical, however, the expected value of the signal sample is the true value. These induced errors can indeed be very large, depending on the location of the trigger time. For example, the induced error at the zero crossing of the reference sinusoid is larger than at any other point.

Similarly, consider kernel-based time encoding of the FRI signal in (7) using an IF-TEM with parameters $\{b, \kappa, \gamma\}$ as

in Figure 2, that provides noisy trigger times as in (17). The local averages, using Lemma 2, are given as $\tilde{y}_n = -b(\tilde{t}_{n+1}' - \tilde{t}_n') + \kappa\gamma$. Hence, the local averages are random variables with $\mathbb{E}[\tilde{y}_n] = \mathbb{E}[-b(\tilde{t}_{n+1}' - \tilde{t}_n') + \kappa\gamma] = -b(t_{n+1}' - t_n') + \kappa\gamma$, and $\text{var}(\tilde{y}_n) = b^2(\text{var}(\nu_{n+1}) + \text{var}(\nu_n)) = 2b^2 \frac{\sigma^2}{12}$. The distribution of the local averages are independent and identically distributed, with the expected value of the local averages equal to the true values.

Further, the jitter in the trigger times appear as perturbations in the forward linear transformations \mathbf{G}_{CT} and \mathbf{G}_{IF} , in the C-TEM and IF-TEM cases, respectively. This effects the conditioning of the matrix and the inversion process to compute the Fourier-series coefficients maybe unstable.

We treat recovery in presence of noise as solving for the Fourier-series coefficients from an arbitrary system of linear measurements of the type $\mathbf{y} = \mathbf{G}\hat{\mathbf{x}}$. The Fourier-series coefficients are then used to find the annihilating filter in the null space of $T_K\hat{\mathbf{x}}$. In the presence of noise, the matrix $T_K\hat{\mathbf{x}}$ may not be rank deficient. In conventional uniform sampling, the matrix $T_K\hat{\mathbf{x}}$ is “denoised” to have rank K using structured low-rank approximations using methods such as Cadzow denoising or its upgraded variants [27], [28]. In case of arbitrary linear measurements like random sampling, Pan et al. [18] proposed a generalisation of the denoising problem to jointly solve for the Fourier-series coefficients and the annihilating filter, by imposing the annihilation equation as a constraint in the optimisation programme. We borrow this idea to solve the system in (16) where the noisy measurements are in time, and further the signal measurements are not necessarily via the identity event operator like in the case of time encoding using IF-TEM.

Consider the system of equations $\mathbf{y} = \mathbf{G}\hat{\mathbf{x}}$, where $\hat{\mathbf{x}} \in \mathbb{C}^N$ is the vector of Fourier-series coefficients, \mathbf{G} is a forward linear transformation and \mathbf{y} are measurements of ψy , where ψ is the event operator of the time-encoding machine. Such a system represents linear systems described in Section IV-A or Section IV-B or the concatenated system as in Section V. In the presence of measurement noise, we wish to recover the Fourier-series coefficients $\hat{\mathbf{x}}$ such that there lies a vector $\mathbf{h} \in \mathbb{C}^{K+1}$, in the null space of the matrix $T_K\hat{\mathbf{x}}$. This vector \mathbf{h} is the annihilating filter of the Fourier-series coefficients, and as discussed in Section II-C, the roots of the annihilating filter are in one-to-one correspondence with the shifts. Further, to avoid the trivial solution for the annihilating filter, we impose regularisation constraints. Experiments in [29] show empirically, that the regularisation $\langle \mathbf{h}^{(0)}, \mathbf{h} \rangle = 1$, where $\mathbf{h}^{(0)} \in \mathcal{CN}(\mathbf{0}, \mathbf{I})$ is used as the initialisation, works best amongst other candidates such as $h_0 = 1$ or $\|\mathbf{h}\|_2 = 1$. Casting this as an optimisation programme:

$$\begin{aligned} & \underset{\hat{\mathbf{x}} \in \mathbb{C}^N, \mathbf{h} \in \mathbb{C}^{K+1}}{\text{minimise}} \|\mathbf{G}\hat{\mathbf{x}} - \mathbf{y}\|_2^2 \\ & \text{subject to } (T_K\hat{\mathbf{x}})\mathbf{h} = \mathbf{0}, \\ & \quad \langle \mathbf{h}, \mathbf{h}^{(0)} \rangle = 1, \end{aligned} \quad (18)$$

we get a nonconvex optimisation programme in the joint variable $(\hat{\mathbf{x}}, \mathbf{h})$. However, the programme is convex in each of the variables. Consider the subprogram by fixing \mathbf{h} . The annihilation constraint can be re-written in the variable $\hat{\mathbf{x}}$ using

the right dual of T_K from Definition 4 to get:

$$\begin{aligned} & \underset{\hat{\mathbf{x}} \in \mathbb{C}^N}{\text{minimise}} \|\mathbf{G}\hat{\mathbf{x}} - \mathbf{y}\|_2^2 \\ & \text{subject to } (R_N \mathbf{h})\hat{\mathbf{x}} = \mathbf{0}, \end{aligned} \quad (19)$$

which is a quadratic programme with a linear equality constraint. The minimiser is given by:

$$\hat{\mathbf{x}} = \boldsymbol{\beta} - (\mathbf{G}^H \mathbf{G})^{-1} (R_N \mathbf{h})^H \boldsymbol{\Gamma}^{-1} (R_N \mathbf{h}) \boldsymbol{\beta}, \quad (20)$$

where $\boldsymbol{\beta} = (\mathbf{G}^H \mathbf{G})^{-1} \mathbf{G}^H \mathbf{y}$ and $\boldsymbol{\Gamma} = [(R_N \mathbf{h}) (\mathbf{G}^H \mathbf{G})^{-1} (R_N \mathbf{h})^H]$. The minimum value of the objective function in (19) can be shown to be $\mathbf{h}^H (T_K \boldsymbol{\beta}) \boldsymbol{\Gamma}^{-1} (T_K \boldsymbol{\beta}) \mathbf{h}$. Therefore, now with the updated $\hat{\mathbf{x}}$ held fixed, minimising the annihilating filter can be cast as:

$$\begin{aligned} & \underset{\mathbf{h} \in \mathbb{C}^{(K+1)}}{\text{minimise}} \mathbf{h}^H (T_K \boldsymbol{\beta}) \boldsymbol{\Gamma}^{-1} (T_K \boldsymbol{\beta}) \mathbf{h} \\ & \text{subject to } \langle \mathbf{h}, \mathbf{h}^{(0)} \rangle = 1, \end{aligned} \quad (21)$$

which is a quadratic programme with an affine constraint. Therefore, the minimiser of (18) can be found using alternative minimisation by solving the subproblems in (19) and (21). Using slack variables, the iterations can be cast as solutions to linear equations (see Proposition 1, [18]). These iterations are empirically known to converge in as few as 50 iterations with multiple random initialisations. Let $(\hat{\mathbf{x}}^*, \mathbf{h}^*)$ be the minimiser obtained. The shifts $\{t_k\}_{k=0}^{K-1}$ can be computed from the roots of \mathbf{h}^* and then, the amplitudes $\{c_k\}_{k=0}^{K-1}$ can be computed using linear least-squares from (8). We summarise this method dubbed ‘‘GenFRI-TEM’’ in Algorithm 1:

Algorithm 1: GenFRI-TEM

Input: Time encoding $\{t'_n\}_{n=1}^L \subset \mathcal{T}(x * g)$ and samples $(\psi(x * g))(\mathcal{T}(x * g))$
Output: Amplitude $\{c_k\}_{k=0}^{K-1}$ and support $\{t_k\}_{k=0}^{K-1}$ parameters of (7)

- 1 Initialise a random vector $\mathbf{h}^{(0)} \in \mathbb{C}^{(K+1)}$
- 2 **repeat**
- 3 **repeat**
- 4 Update $\hat{\mathbf{x}}$ by solving (19)
- 5 Update \mathbf{h} by solving (21)
- 6 **until** $\|\mathbf{y} - \mathbf{G}\hat{\mathbf{x}}\|_2^2 \leq \eta$ or max iterations
- 7 **until** number of initialisations
- 8 Find the roots of \mathbf{h} to find $\{t_k\}_{k=0}^{K-1}$
- 9 Compute $\{c_k\}_{k=0}^{K-1}$ by solving the linear system in (8).

VII. EXPERIMENTS AND RESULTS

In this Section, we demonstrate the working of the algorithm with simulated experiments.

A. Perfect Recovery using Noise-free Single Channel Measurements

We analyse the performance of the reconstruction algorithm in the noise-free setting. We consider a τ -periodic FRI signal as in (7) with $\tau = 1$, and $K = 5$ Dirac impulses that are randomly initialised. We use the SoS kernel [17]:

$$g(t) = \text{rect}\left(\frac{t}{\tau}\right) D_K\left(\frac{2\pi t}{\tau}\right), \quad (22)$$

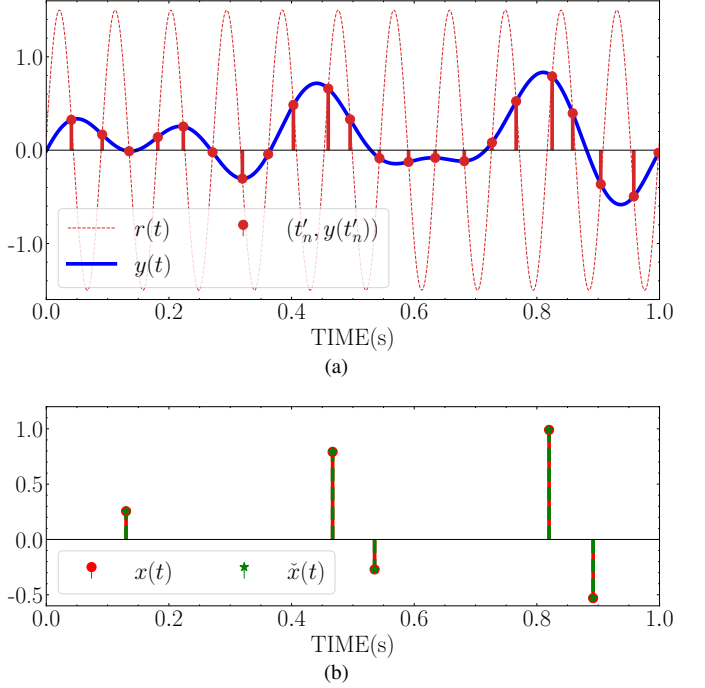


Fig. 5. [Colour online] Time encoding and reconstruction using C-TEM: (a) the filtered signal $y(t)$, the reference signal $r(t)$ and the corresponding trigger times; and (b) the input stream of Dirac impulses $x(t)$ and the reconstruction $\check{x}(t)$.

where $D_K(t) = \frac{\sin((K+1/2)t)}{\sin(t/2)}$ is the Dirichlet kernel, as the sampling kernel for time encoding as in Figure 3. This kernel provides access to the critical $2K + 1$ Fourier-series coefficients.

First, we consider time encoding of the filtered signal using a C-TEM with sinusoidal reference signal $r(t) = 1.5 \cos(2\pi \cdot 11 \cdot t)$. This critically satisfies Proposition 1. We use Algorithm 1 to recover the signal, with 50 initialisations and 50 iterations for each initialisation. Figure 5(a) shows the filtered signal $y(t) = (x * g)(t)$, the sinusoidal reference signal $r(t)$, and the trigger time, signal sample pairs $(t'_n, y(t'_n))$, $n = 1, \dots, 22$. Figure 5(b) shows the FRI signal $x(t)$ and the reconstruction $\check{x}(t)$. The reconstruction is perfect upto numerical precision.

Second, we consider time encoding of the filtered signal using IF-TEM with parameters $b = 1.5$, $\kappa = 1$ and $\gamma = 0.09$ such that Proposition 2 is satisfied. We use Algorithm 1 to recover the signal, with 50 initialisations and 50 iterations for each initialisation. Figure 6(a) shows the filtered signal $y(t) = (x * g)(t)$, the output of the integrator $v(t)$, and the trigger times t'_n , $n = 1, \dots, 17$. Figure 6(b) shows the FRI signal $x(t)$ and the reconstruction $\check{x}(t)$. The reconstruction is perfect upto numerical precision.

B. Perfect Recovery using Noise-free Multichannel Measurements

We analyse the performance of the reconstruction algorithm in the noise-free setting with multichannel measurements. We consider a τ -periodic FRI signal as in (7) with $\tau = 1$, and $K = 5$ Dirac impulses that are randomly initialised. We use the SoS kernel as in (22) as the sampling kernel for time encoding as in Figure 3. This provides access to the critical $2K + 1$ Fourier-series coefficients.

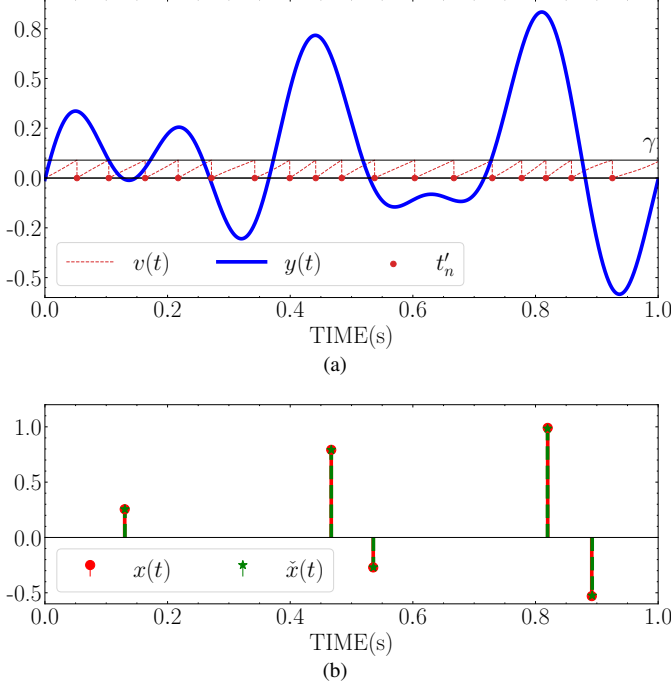


Fig. 6. [Colour online] Time encoding and reconstruction using IF-TEM: (a) the filtered signal $y(t)$, the output of the integrator $v(t)$ and the corresponding trigger times; and (b) the input stream of Dirac impulses $x(t)$ and the reconstruction $\check{x}(t)$.

First, we consider time encoding of the filtered signal using $C = 2$ C-TEMs with sinusoidal reference signals $r^{(1)}(t) = 1.5 \cos(2\pi \cdot 5.5 \cdot t + \phi_r^{(1)})$ and $r^{(2)}(t) = 1.5 \cos(2\pi \cdot 5.5 \cdot t + \phi_r^{(2)})$, where $\phi_r^{(1)}$ and $\phi_r^{(2)}$ are picked from a uniform distribution in the interval $[0, 2\pi]$. This critically satisfies Proposition 3. Note the reduction in sampling requirement in each channel. We use Algorithm 1 to recover the signal, with 50 initialisations and 50 iterations for each initialisation. Figure 7(a) shows the filtered signal $y(t) = (x * g)(t)$, the sinusoidal reference signals $r^{(1)}(t)$ and $r^{(2)}(t)$, and the corresponding trigger time, signal sample pairs. Figure 7(b) shows the FRI signal $x(t)$ and the reconstruction $\check{x}(t)$. The reconstruction is perfect upto numerical precision.

Second, we consider time encoding of the filtered signal using $C = 2$ IF-TEMs with parameters $b^{(1)} = b^{(2)} = 1.5$, $\kappa^{(1)} = 1$, $\kappa^{(2)} = 0.82$, $\gamma^{(1)} = 0.18$, $\gamma^{(2)} = 0.2$, and initial values of the integrators offset by 0.07, such that Proposition 4 is satisfied. Note the reduction in sampling requirement in each channel. We use Algorithm 1 to recover the signal, with 50 initialisations and 50 iterations for each initialisation. Figure 8(a) shows the filtered signal $y(t) = (x * g)(t)$, the output of the integrators $v^{(1)}(t)$, $v^{(2)}(t)$, and the corresponding trigger times. Figure 8(b) shows the FRI signal $x(t)$ and the reconstruction $\check{x}(t)$. The reconstruction is perfect upto numerical precision.

C. Recovery from Noisy Measurements

We analyse the performance of the reconstruction algorithm in the presence of jitter in the measurements. We consider a τ -periodic FRI signal as in (7) with $\tau = 1$, and $K = 5$ Dirac impulses that are randomly initialised. We use the SoS kernel as in (22) for kernel-based time encoding as in Figure 3.

First, we consider time encoding using C-TEM and IF-TEM identical to Section VII-B, now with jitter in the trigger times drawn from a uniform distribution with $\sigma = 10^{-3}$ (see Section VI). Time encoding using C-TEM and IF-TEM are identical to Figures 5(a) and 6(a), respectively. We use Algorithm 1 to recover the signal, with 50 initialisations and 50 iterations for each initialisation. Figures 9(a) and 9(b) show the FRI signal $x(t)$ and the reconstruction $\check{x}(t)$ from the noisy C-TEM and IF-TEM measurements, respectively. In both cases, the error in estimating the shifts $\frac{1}{K} \sum_{k=0}^{K-1} (t_k - \check{t}_k)^2$, where $\{\check{t}_k\}_{k=0}^{K-1}$ is of the order of 10^{-5} .

Next, we perform Monte-Carlo simulations to validate the performance across a range of values for σ in $\{10^{-6}, 10^{-5}, 10^{-4}, 10^{-3}, 10^{-2}, 10^{-1}, 10^0\}$. We consider the reconstruction of the same FRI signal using Algorithm 1, Prony's method (see Section II-C) and Cadzow Plug-and-Play Gradient Descent (CPGD) [30]. We consider the error in shifts as $\frac{1}{K} \sum_{k=0}^{K-1} (t_k - \check{t}_k)^2$, where $\{\check{t}_k\}_{k=0}^{K-1}$ are the estimated shifts, over 100 realisations of jitter, from C-TEM and IF-TEM measurements, respectively.

Figure 10 shows the variation of the error in shifts with jitter width σ . With lower values of jitter width, Algorithm 1 performs several orders of magnitude better than the counterparts. As the jitter width increases, the error in shifts begin to be comparable between the recovery methods.

Figures 11 and 12 show the mean of the recovered positions as compared to the true position, from C-TEM and IF-TEM measurements respectively. With smaller values of jitter width, the recovery of shifts using Algorithm 1 are consistent with the true shifts. With larger values of jitter width, the recovered shifts have an additional bias.

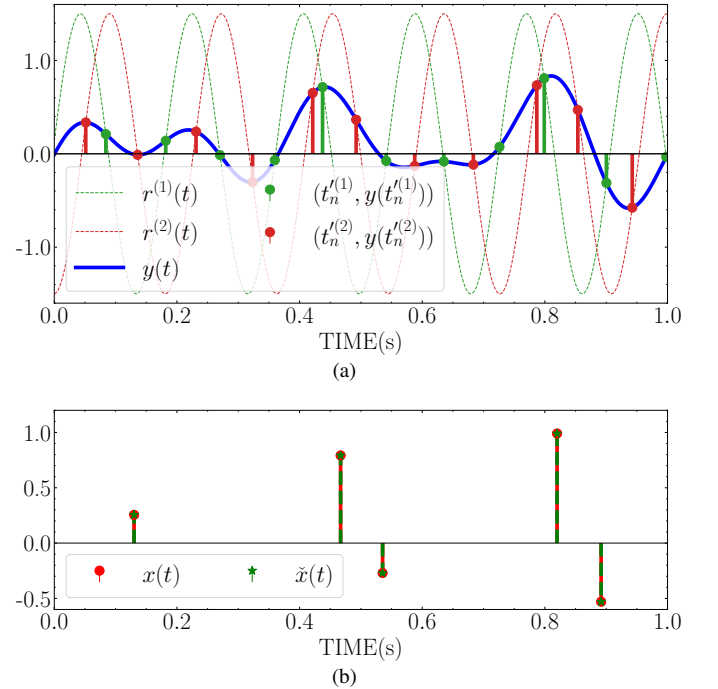
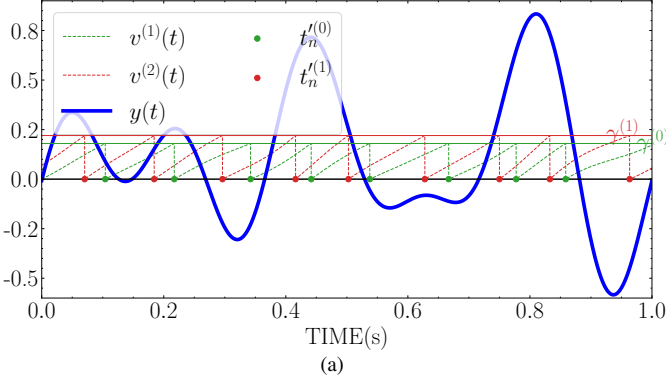
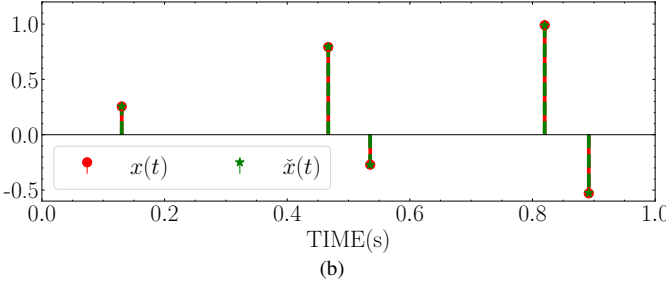


Fig. 7. [Colour online] Time encoding and reconstruction using C-TEM: (a) the filtered signal $y(t)$, the reference signals $r^{(1)}(t)$, $r^{(2)}(t)$ and the corresponding trigger times; and (b) the input stream of Dirac impulses $x(t)$ and the reconstruction $\check{x}(t)$.



(a)

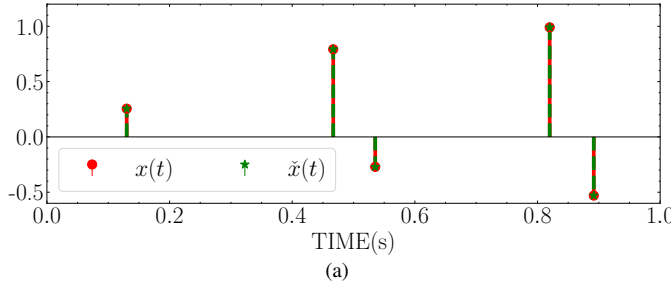


(b)

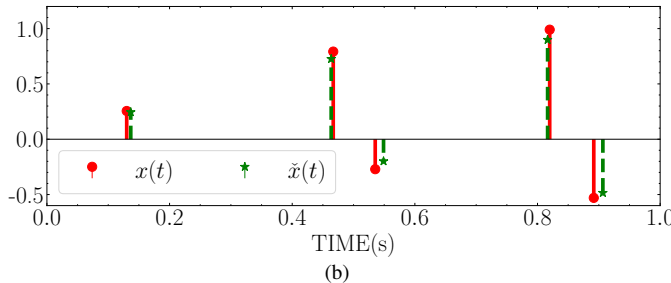
Fig. 8. [Colour online] Time encoding and reconstruction using IF-TEM: (a) the filtered signal $y(t)$, the output of the integrators $v^{(1)}(t)$, $v^{(2)}(t)$ and the corresponding trigger times; and (b) the input stream of Dirac impulses $x(t)$ and the reconstruction $\hat{x}(t)$.

VIII. CONCLUSIONS

We considered time encoding of FRI signals, in specific, using the crossing-time-encoding machine and the integrate-and-fire time-encoding machine. We analysed time encoding in the frequency domain, and showed the measurements of the FRI signal obtained from time-encoding machines, using a suitable sampling kernel, can be set as a linear system of equations with the Fourier-series coefficients as unknowns. In

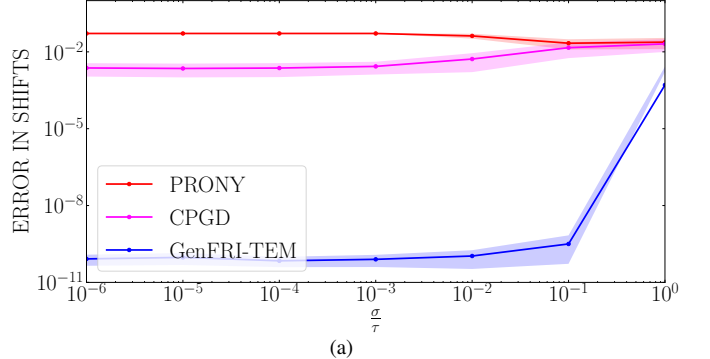


(a)

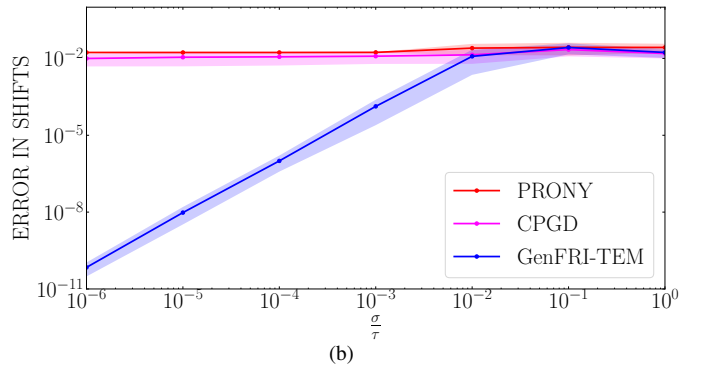


(b)

Fig. 9. [Colour online] Time encoding and reconstruction using noisy TEMs: (a) the input stream of Dirac impulses $x(t)$ and the reconstruction $\hat{x}(t)$ using C-TEM; and (b) the input stream of Dirac impulses $x(t)$ and the reconstruction $\hat{x}(t)$ using IF-TEM.



(a)



(b)

Fig. 10. [Colour online] Error in shifts varying with the jitter width σ : (a) corresponds to reconstruction from C-TEM measurements; and (b) corresponds to measurements from IF-TEM measurements. The solid line shows the mean of the errors and the shaded region captures 1 standard deviation. The results are averaged over 100 realisations of jitter. Both axes are in log scale.

the noise-free case, the linear system of equations has a unique solution and standard techniques of FRI signal recovery can be applied. We then extended the analysis to multichannel time encoding and showed the sampling requirement in each channel can be reduced. We analysed the effect of measurement noise which is modelled as jitter in the time encoding. To this end, we proposed an optimisation algorithm inspired by the Generalised FRI framework to jointly solve for the Fourier-series coefficients and the annihilating filter. We presented sufficient conditions for perfect reconstruction of FRI signals together with simulations to validate the claims.

APPENDIX A PROOF OF LEMMA 1

Proof. Let $y : [0, \tau] \rightarrow \mathbb{R}$ be continuous and differentiable be sampled using a C-TEM with reference $r(t) = A_r \cos(2\pi f_r t)$ with $A_r \geq \|y\|_\infty$. Consider the partition of the interval $[0, \tau]$ into smaller intervals of $\mathcal{U}_m = \left[m \frac{1}{2f_r}, (m+1) \frac{1}{2f_r}\right]$, where $m = 1, 2, \dots$. Note that $\mathcal{U}_m \cap \mathcal{U}_{m+1} = \emptyset$ and $\mathcal{U}_m \cap \mathcal{U}_{m+1} = [0, \tau]$. For every m , we have, $(r(m \frac{1}{2f_r}) - y(m \frac{1}{2f_r})) \cdot (r((m+1) \frac{1}{2f_r}) - y((m+1) \frac{1}{2f_r})) < 0$, i.e., the sign of the difference signal $(r - y)$ changes once in the interval \mathcal{U}_m . Since r is continuous and differentiable, $r - y$ is continuous and differentiable, and hence, using Bolzano's intermediate value theorem, $\exists t'_n \in \mathcal{U}_m$ such that $s(t'_n) - y(t'_n) = 0$, i.e., in the interval of half a period of the signal r , the

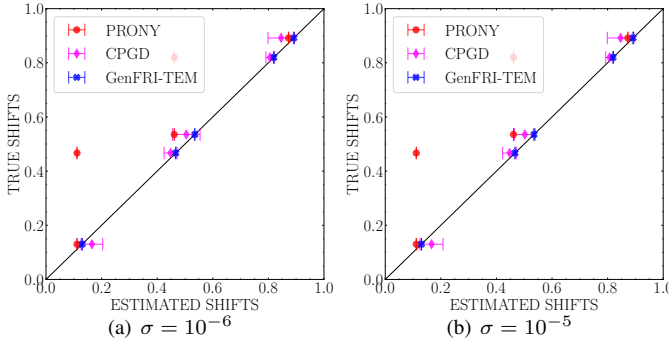
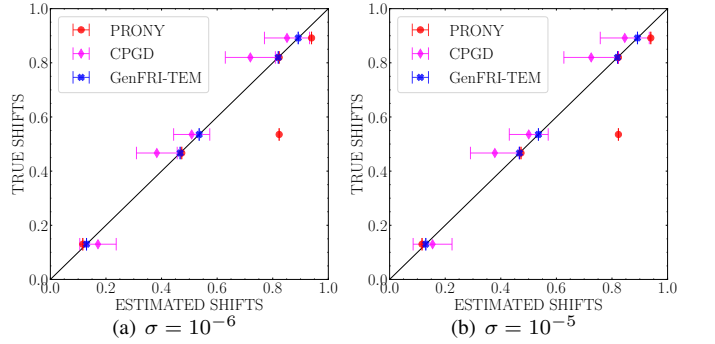
(a) $\sigma = 10^{-6}$ (b) $\sigma = 10^{-5}$ (c) $\sigma = 10^{-2}$ (d) $\sigma = 1$ (a) $\sigma = 10^{-6}$ (b) $\sigma = 10^{-5}$ (c) $\sigma = 10^{-2}$ (d) $\sigma = 1$

Fig. 11. [Colour online] Comparison of recovered shifts from C-TEM measurements to the true shifts, for varying values of jitter width σ : the horizontal axis plots the estimated shifts and the vertical axis plots the true shifts. Each marker corresponds to the mean value recovered of one shift, with one standard deviation cap. The closer the marker is to the straight line with unit slope, the better is the recovery.

signal $(y - r)$ crosses zero at least once at t'_n . Therefore, $\sup_{n \in \mathbb{Z}} |t'_{n+1} - t'_n| < \frac{1}{f_s}$. \square

APPENDIX B PROOF OF LEMMA 2

This is an adaptation of the proof given in [5], where the authors consider a practical model with the additional refractory period. In our case, we assume the IF-TEM to be ideal and set the refractory period to be zero.

Proof. Let y be the input to the IF-TEM with parameters $\{b, \kappa, \gamma\}$, and let $t_n \in \mathcal{T}y$. According to the working of the IF-TEM, the next trigger time occurs at a point t_{n+1} such that:

$$\frac{1}{\kappa} \int_{t_n}^{t_{n+1}} (y(t) + b) dt = \gamma. \quad (23)$$

The result follows:

$$\int_{t_n}^{t_{n+1}} y(t) dt = -b(t_{n+1} - t_n) + \kappa\gamma. \quad (24)$$

\square

APPENDIX C PROOF OF COROLLARY 1

Proof. Let y be the input to the IF-TEM with parameters $\{b, \kappa, \gamma\}$, and additionally, let $\|y\|_\infty < b$. We have:

$$-\int_{t_n}^{t_{n+1}} \|y\|_\infty dt \leq \int_{t_n}^{t_{n+1}} y(t) dt \leq \int_{t_n}^{t_{n+1}} \|y\|_\infty dt, \quad (25)$$

Fig. 12. [Colour online] Comparison of recovered shifts from IF-TEM measurements to the true shifts, for varying values of jitter width σ : the horizontal axis plots the estimated shifts and the vertical axis plots the true shifts. Each marker corresponds to the mean value recovered of one shift, with one standard deviation cap. The closer the marker is to the straight line with unit slope, the better is the recovery.

for any $t_n \leq t_{n+1}$. In particular, when $t_n, t_{n+1} \in \mathcal{T}y$, using (24), and carrying out the integrals on the L.H.S and R.H.S, we get:

$$-\|y\|_\infty(t_{n+1} - t_n) \leq -b(t_{n+1} - t_n) + \kappa\gamma \leq \|y\|_\infty(t_{n+1} - t_n), \quad (26)$$

and consequently, the result follows:

$$\frac{\kappa\gamma}{b + \|y\|_\infty} \leq t_{n+1} - t_n \leq \frac{\kappa\gamma}{b - \|y\|_\infty}. \quad (27)$$

\square

APPENDIX D PROOF OF LEMMA 3

Proof. Consider the case where $L = N$, i.e., the matrix \mathbf{G}_{CT} is a square matrix. In this case, we will show that the matrix has a nonzero determinant, and $\text{rank}(\mathbf{G}_{CT}) = N$. For the case when $L > N$, adding rows to the $N \times N$ matrix cannot decrease the rank, and hence they have full column rank. In the particular case when the matrix is square, using the properties of determinants:

$$\det(\mathbf{G}_{CT}) = \prod_{n=1}^L e^{-jM\omega_0 t'_n} \cdot \det(\mathbf{F}),$$

where the matrix $\mathbf{F} \in \mathbb{C}^{L \times N}$ is given by:

$$\mathbf{F} = \begin{bmatrix} 1 & e^{j\omega_0 t'_1} & \dots & e^{j2M\omega_0 t'_1} \\ 1 & e^{j\omega_0 t'_2} & \dots & e^{j2M\omega_0 t'_2} \\ \vdots & \vdots & & \vdots \\ 1 & e^{j\omega_0 t'_L} & \dots & e^{j2M\omega_0 t'_L} \end{bmatrix},$$

which is a Vandermonde matrix. Using the Definition 1, the set $\{t'_n\}_{n=1}^N$ has increasing and distinct entries. Further since $t'_1, \dots, t'_N \in [0, \tau]$, the set $\{e^{j\omega_0 t'_n}\}_{n=1}^L$ has distinct entries. Using the properties of Vandermonde matrices, $\det(\mathbf{F}) \neq 0$ whenever $L \geq N$ and each term in the product $\prod_{n=1}^N e^{-jL\omega_0 t'_n}$ is nonzero. Hence, $\det(\mathbf{G}_{\text{CT}}) \neq 0$ whenever $L \geq N$. \square

APPENDIX E PROOF OF PROPOSITION 1

Proof. Let x be the τ -periodic FRI signal that is time encoded using a sampling kernel g and a C-TEM with reference $r(t) = A_r \cos(2\pi f_r t)$. The signal is characterised by the $2K$ parameters $\{c_k, t_k\}$, and from Section II-C, the parameters can be recovered using $2K + 1$ Fourier-series measurements.

Let the sampling kernel g satisfy (10). Then, via (12), and with $M = K$, $2K + 1$ contiguous Fourier-series coefficients are revealed via a linear system. Using Lemma 3, the linear system has a unique left inverse when $L \geq 2K + 1$. Therefore, the C-TEM must sample such that $L \geq 2K + 1$.

Let the amplitude of the reference of the C-TEM satisfy $A_r \geq \|x * g\|_\infty$. Using Lemma 1, we obtain at least one sample in every interval $\left[m \frac{1}{2f_r}, (m+1) \frac{1}{2f_r}\right]$, $m = 1, 2, \dots$. Therefore, to obtain $2K + 1$ samples in the interval $[0, \tau]$, $(2K + 1) \frac{1}{f_s} < \tau$.

Remark. The last part of this proof and Lemma 1 do not account for the structure of the input signal, other than the fact that $2K + 1$ samples are required. Hence, the number of samples obtained is usually twice than necessary. \square

APPENDIX F PROOF OF LEMMA 4

Proof. Consider the matrix \mathbf{G}_{IF} as defined in (15). Note, from the derivation (14), the matrix is the resultant of a finite-difference operation on a matrix of the type \mathbf{G}_{CT} . Particularly, we can write \mathbf{G}_{IF} as a product of the finite-difference matrix:

$$\mathbf{D} = \begin{bmatrix} 1 & -1 & \dots & 0 \\ 0 & 1 & \dots & 0 \\ \vdots & \vdots & \ddots & \vdots \\ 0 & 0 & \dots & -1 \end{bmatrix} \in \mathbb{C}^{(L-1) \times L}, \quad (28)$$

and the matrix $\tilde{\mathbf{G}}_{\text{CT}} \in \mathbb{C}^{L \times N}$ defined by:

$$\tilde{\mathbf{G}}_{\text{CT}} = \begin{bmatrix} e^{-jM\omega_0 t_1} & \dots & t_1 & \dots & e^{jM\omega_0 t_1} \\ \vdots & \ddots & \vdots & \ddots & \vdots \\ e^{-jM\omega_0 t_L} & \dots & t_L & \dots & e^{jM\omega_0 t_L} \end{bmatrix}. \quad (29)$$

For brevity and ease of notation, the primes on the variables t_ℓ have been dropped. The notation $\tilde{\mathbf{G}}_{\text{CT}}$ is used to show the matrix is similar in definition to (13). We are interested in solutions to the equation $\mathbf{G}_{\text{IF}}\mathbf{u} = \mathbf{D}\tilde{\mathbf{G}}_{\text{CT}}\mathbf{u} = \mathbf{0}$, and want to show the set of \mathbf{u} that satisfy the equation has only the all-zero vector.

Note that the dimension of the null space of the finite-difference matrix is 1, and has vectors of the form $\alpha \mathbb{1}$, where $\alpha \in \mathbb{C}$ and $\mathbb{1} \in \mathbb{C}^L$ is the all-ones vector. Therefore, the

problem reduces to finding the set of vectors \mathbf{u} that satisfy $\tilde{\mathbf{G}}_{\text{CT}}\mathbf{u} = \alpha \mathbb{1}$. Any entry in the equation has the form:

$$\sum_{\substack{m=-M \\ m \neq 0}}^M u_m e^{jm\omega_0 t_\ell} + u_0 t_\ell = \alpha. \quad (30)$$

The set of vectors \mathbf{u} that satisfy (30) for $\ell = 1, 2, \dots, L$ is empty, whenever $L > N$. This is because, solutions to (30) with rearrangement, can be written as solutions the coefficients of fitting an M th-degree trigonometric polynomial to a line that intersects exactly at the L points t_1, t_2, \dots, t_L . This problem has no solutions whenever $L > N$, as the M th-degree polynomial can have only exactly N such solutions. \square

APPENDIX G PROOF OF PROPOSITION 2

Proof. Let x be the τ -periodic FRI signal that is time encoded using a sampling kernel g and an IF-TEM with parameters $\{b, \kappa, \gamma\}$ as in Figure 3. The filtered signal $y = (x * g)$ is the input to the IF-TEM. Let $t'_1 \in [0, \tau]$ be the first time instant. To further obtain $(L-1)$ time instants in $[0, \tau]$, using Corollary 1, we have:

$$t'_1 + (L-1) \frac{\kappa\gamma}{b - \|y\|_\infty} < \tau. \quad (31)$$

Without loss of generality, we assume the initial output of the integrator $v(0) = 0$. The maximum time taken to produce the first time instant must satisfy

$$\begin{aligned} \gamma &= v(t'_1) = \frac{1}{\kappa} \int_0^{t'_1} \min_\nu(b + y(\nu)) d\nu, \\ &\geq \frac{1}{\kappa} \int_0^{t'_1} (b - \|y\|_\infty) d\nu = \frac{1}{\kappa} (b - \|y\|_\infty) t'_1, \\ &\implies t'_1 \leq \frac{\kappa\gamma}{b - \|y\|_\infty}. \end{aligned}$$

Using this in (31), we have:

$$\frac{\kappa\gamma}{b - \|x * g\|_\infty} < \frac{\tau}{L}, \quad (32)$$

i.e., to obtain $L \geq (2K + 1)$ time instants in $[0, \tau]$ (32) must hold. Further, with $L \geq (2K + 1)$, using Lemma 4, the system $\bar{y} = \mathbf{G}_{\text{IF}}\mathbf{x}$ admits a unique least-squares solution. The $(2K + 1)$ Fourier-series coefficients are sufficient for estimation of the unknown support and amplitudes using Prony's method (Section II-C) and hence, sufficiently represent the τ -periodic FRI signal. \square

REFERENCES

- [1] M. Unser, "Sampling-50 years after Shannon," *Proc. IEEE*, vol. 88, no. 4, pp. 569–587, 2000.
- [2] C. E. Shannon, "Communication in the presence of noise," *Proceedings of the IRE*, vol. 37, no. 1, pp. 10–21, 1949.
- [3] E. D. Adrian, "The basis of sensation: The actions of sense organs," Tech. Rep., Christophers, London, 1928.
- [4] A. N. Burkitt, "A review of the integrate-and-fire neuron model: I. Homogeneous synaptic input," *Biological Cybernetics*, vol. 95, no. 1, pp. 1–19, 2006.
- [5] A. A. Lazar, "Time encoding with an integrate-and-fire neuron with a refractory period," *Neurocomputing*, vol. 58, pp. 53–58, 2004.
- [6] C. Brandli, R. Berner, M. Yang, S. C. Liu, and T. Delbrück, "A 240×180 130 dB 3 μ s latency global shutter spatiotemporal vision sensor," *IEEE J. Solid-State Circuits*, vol. 49, no. 10, pp. 2333–2341, 2014.

- [7] T. Delbrück, B. Linares-Barranco, E. Culurciello, and C. Posch, “Activity-driven, event-based vision sensors,” in *Proc. IEEE Int. Symp. Circuits Syst. (ISCAS)*, 2010, pp. 2426–2429.
- [8] R. Wiley, “Recovery of bandlimited signals from unequally spaced samples,” *IEEE Trans. Commun.*, vol. 26, no. 1, pp. 135–137, 1978.
- [9] I. W. Sandberg, “On the properties of some systems that distort signals,” *Bell System Technical Journal*, vol. 42, no. 5, pp. 2033–2046, 1963.
- [10] K. Adam, A. Scholefield, and M. Vetterli, “Sampling and reconstruction of bandlimited signals with multi-channel time encoding,” *IEEE Trans. Signal Process.*, vol. 68, pp. 1105–1119, 2020.
- [11] A. Aldroubi and K. Gröchenig, “Nonuniform sampling and reconstruction in shift-invariant spaces,” *SIAM Review*, vol. 43, no. 4, pp. 585–620, 2001.
- [12] D. Gontier and M. Vetterli, “Sampling based on timing: Time encoding machines on shift-invariant subspaces,” *Appl. Comput. Harmon. Anal.*, vol. 36, no. 1, pp. 63–78, 2014.
- [13] Y. M. Lu and M. N. Do, “A theory for sampling signals from a union of subspaces,” *IEEE Trans. Signal Process.*, vol. 56, no. 6, pp. 2334–2345, 2008.
- [14] M. Vetterli, P. Marziliano, and T. Blu, “Sampling signals with finite rate of innovation,” *IEEE Trans. Signal Process.*, vol. 50, no. 6, pp. 1417–1428, June 2002.
- [15] O. Bar-Ilan and Y. C. Eldar, “Sub-Nyquist radar via Doppler focusing,” *IEEE Trans. Signal Process.*, vol. 62, no. 7, pp. 1796–1811, Apr. 2014.
- [16] S. Rudresh and C. S. Seelamantula, “Finite-rate-of-innovation-sampling-based super-resolution radar imaging,” *IEEE Trans. Signal Process.*, vol. 65, no. 19, pp. 5021–5033, 2017.
- [17] R. Tur, Y. C. Eldar, and Z. Friedman, “Innovation rate sampling of pulse streams with application to ultrasound imaging,” *IEEE Trans. Signal Process.*, vol. 59, no. 4, pp. 1827–1842, Apr. 2011.
- [18] H. Pan, T. Blu, and M. Vetterli, “Towards generalized FRI sampling with an application to source resolution in radioastronomy,” *IEEE Trans. Signal Process.*, vol. 65, no. 4, pp. 821–835, 2016.
- [19] R. Alexandru and P. L. Dragotti, “Reconstructing classes of non-bandlimited signals from time-encoded information,” *arXiv preprint arXiv:1905.03183*, 2019.
- [20] B.F Logan Jr, “Information in the zero crossings of bandpass signals,” *Bell System Technical Journal*, vol. 56, no. 4, pp. 487–510, 1977.
- [21] I. Bar-David, “An implicit sampling theorem for bounded bandlimited functions,” *Inform. Contr.*, vol. 24, no. 1, pp. 36–44, 1974.
- [22] C.S. Seelamantula, “A sub-nyquist sampling method for computing the level-crossing-times of an analog signal: Theory and applications,” in *Proc. IEEE Int. Conf. Signal Process., Comm. (SPCOM)*, 2010, pp. 1–5.
- [23] G. R. deProny, “Essai experimental et analytique: Sur les lois de la dilatabilité de fluides élastiques et sur celles de la force expansive de la vapeur de l'eau et de la vapeur de l'alcool, à différentes températures,” *J. de l'Ecole Polytechnique*, vol. 1, no. 2, pp. 24–76, 1795.
- [24] T. Blu, P. L. Dragotti, M. Vetterli, P. Marziliano, and L. Coulot, “Sparse sampling of signal innovations,” *IEEE Signal Process. Mag.*, vol. 25, no. 2, pp. 31–40, Mar. 2008.
- [25] S. Mulleti and C. S. Seelamantula, “Paley–Wiener characterization of kernels for finite-rate-of-innovation sampling,” *IEEE Trans. Signal Process.*, vol. 65, no. 22, pp. 5860–5872, 2017.
- [26] P. L. Dragotti, M. Vetterli, and T. Blu, “Sampling moments and reconstructing signals of finite rate of innovation: Shannon meets Strang-Fix,” *IEEE Trans. Signal Process.*, vol. 55, no. 5, pp. 1741–1757, May 2007.
- [27] J. A. Cadzow, “Signal enhancement – A composite property mapping algorithm,” *IEEE Trans. Acoust., Speech, Signal Process.*, vol. 36, no. 1, pp. 49–62, 1988.
- [28] L. Condat and A. Hirabayashi, “Cadzow denoising upgraded: A new projection method for the recovery of dirac pulses from noisy linear measurements,” *Sampl. Theory Signal Image Process.*, vol. 14, no. 1, pp. 17–47, 2015.
- [29] Z. Doğan, C. Gilliam, T. Blu, and D. Van De Ville, “Reconstruction of finite rate of innovation signals with model-fitting approach,” *IEEE Trans. Signal Process.*, vol. 63, no. 22, pp. 6024–6036, 2015.
- [30] M. Simeoni, A. Besson, P. Hurley, and M. Vetterli, “Cpgd: Cadzow plug-and-play gradient descent for generalised fri,” *IEEE Trans. Signal Process.*, vol. 69, pp. 42–57, 2021.